ISSN 1027-5495. Functional Materials, 25, No.2 (2018), p. 208-217.
doi:https://doi.org/10.15407/fm25.02.208

Influence of crystal growth conditions and carbothermal treatment on activator charge state in Ti:sapphire

S.V.Nizhankovskiy, N.S.Sidelnikova, V.V.Baranov

Institute for Single Crystals, STC "Institute for Single Crystals",
National Academy of Sciences of Ukraine,
60 Nauky Ave., 61178 Kharkiv, Ukraine

Received July 25, 2017

Presented are the results of comparative studies of the influence of carbothermal treatment of the raw material (Al_2O_3 and TiO_2 powders) and reducing properties of the growth medium on the charge state of titanium ions in Al_2O_3:Ti crystals. It is shown that carbothermal treatment at temperatures of 1700–1800°C makes it possible to additionally decrease the relative content of titanium in the charge state Ti^{4+} by 2.5–3 times.
Keywords: Al_2O_3 , TiO_2, carbothermal treatment.

Приведены результаты сравнительных исследований влияния восстановительных свойств среды выращивания и карботермической обработки шихты на зарядовое состояние ионов титана в кристаллах Al_2O_3:Ti. Показано, что предварительная карботермическая обработка шихты при температурах 1700–1800°C позволяет дополнительно понизить в кристаллах содержание активатора в зарядовом состоянии Ti^{4+} в 3–4 раза.

Вплив умов вирощування та карботермічної обробки на зарядовий стан активатора у кристалах Ti:сапфіру. *С.В.Нижанківський, Н.С.Сидельникова, В.В.Баранов.*
Наведено результати порівняльних досліджень впливу відновлювальних властивостей середовища вирощування і карботермічної обробки шихти на зарядовий стан іонів титану у кристалах Al_2O_3:Ti. Показано, що попередня карботермічна обробка шихти при температурах 1700–1800°C дозволяє додатково знизити у кристалах вміст активатора у зарядовому стані Ti^{4+} у 3–4 рази.

1. Introduction

Laser efficiency of Ti:sapphire essentially depends on the value of optical loss at laser generation wavelengths in (650–1100 nm) region. As established in [1–4], Ti:sapphire has a wide absorption band with a maximum at ~ 820 nm caused by the presence of the complex centers Ti^{3+}–Ti^{4+} in the crystal. The generally accepted criterion of laser efficiency for this crystal is the value of FOM (figure of merit), i.e. the ratio between the values of optical absorption in the pumping region and of absorption at the generation maximum (~ 800 nm). The intensity of parasitic absorption is defined by the concentration of the pairs Ti^{3+}–Ti^{4+} which depends on the total content of titanium and its relative content in the charge state Ti^{4+}. In its turn, the latter value depends on the partial pressure of oxygen in the technological crystal growth medium, thermal treatment and impurity composition.

The most widespread method for diminution of Ti^{4+} concentration is reducing annealing of the as-grown crystals which permits to raise the value of FOM up to 200–250 and higher for weakly activated crystals with the concentration of titanium not exceeding 0.02–0.05 wt.%. However,

with the rise of the size of the crystal elements such a method becomes inefficient, since the required annealing duration increases as the square of the linear size of the element, and is accompanied with essential technological difficulties. Moreover, the increase of the activator concentration in the crystals considerably lowers the value of FOM. For small (up to 5–10 mm) crystals with the concentration of titanium not lower than 0.07–0.15 wt.%, the value of FOM normally achieved by means of the annealing is ≈100–150.

In the described method the reduction degree for titanium ions ($Ti^{4+} \rightarrow Ti^{3+}$) is defined by the equilibrium constant of the oxidation-reduction reaction [4]:

$$3Ti_{Al}^{3+} + \frac{3}{4}O_2(gas) \leftrightarrow 3Ti_{Al}^{4+} + V_{Al}^{3-} + \frac{3}{2}O_0, \quad (1)$$

which depends on the partial pressure of oxygen above the crystal and the concentration of anionic vacancies in the crystal [5]:

$$K_{ox,V}^{Ti} = \frac{[Ti_{Al}^{4+}]^3}{[Ti_{Al}^{3+}]^3}[V_{Al}^{3-}]P_{O_2}^{-3/4}, \quad (2)$$

where $[Ti_{Al}^{3+}]$ and $[Ti_{Al}^{4+}]$ is the concentration of Ti ions in the charge state 3^+ and 4^+, respectively; $[V_{Al}^{3-}]$, the concentration of anionic vacancies; P_{O_2}, the partial pressure of oxygen in the growth medium. As follows from (2), the reduction degree for titanium ions $Ti^{4+} \rightarrow Ti^{3+}$ increases with the rise of the concentration of anionic vacancies and diminution of the partial pressure of oxygen. At the same time, as established earlier [6], a considerable increase of the concentration of anionic vacancies in inactivated sapphire crystals can be achieved not only due to reduction of the partial pressure of oxygen in the vapor phase of Al_2O_3, but also by means of carbothermal reduction (CTR) of the raw material. In the latter case carbon additive is introduced in the form of fine-dispersed powder of graphite (soot, etc.) or aluminium carbide (Al_4C_3). Thereat, the concentration of anionic vacancies in the crystals considerably rises (up to ~ 10^{18} cm^{-3}), that can be estimated from the intensity of the optical absorption bands for F and F^+-centers. It may be expected that CTR will promote more intense $Ti^{4+} \rightarrow Ti^{3+}$ reduction and allow to decrease the relative concentration of Ti^{4+} in Al_2O_3:Ti crystals. Reported in [7] are the results on the growth of carbon-doped Ti:sapphire crystals by the Kyropoulos method which speak for this assumption. However, the presence of carbon at the crystal growth stage may considerably raise gas formation in the melt and lead to the formation of optical defects. In the developed approach CTR is used at the preliminary stage of the initial material treatment which must be optimized for the obtaining of the crystals with high optical quality and low absorption in the range of laser generation wavelengths.

The present work was aimed at comparative studies of the influence of the reducing properties of the growth medium and CTR on the content of the activator in the charge state Ti^{4+} and optical absorption in Ti:sapphire.

2. Experimental

Sapphire crystals with ≈7–8·10^{-4} wt. % content of residual titanium additive and Ti:sapphire crystals containing ≈0.06 wt. % of titanium with the dimensions 100–175×100–175×40 mm^3 were grown from molybdenum crucibles in a furnace with carbon graphite thermal insulation [8] in low-pressure (13–40 Pa, $P_{H_2}/P_{CO} \approx 0.01–0.04$) CO + H_2medium and in Ar atmosphere (1.1·10^5 Pa–1.3·10^5 Pa), at the partial pressure of the reducing component P_{CO}/P_{H_2} ~ 130–400 Pa, $P_{H_2}/P_{O_2} \approx 0.01–0.1$. The concentration of CO, H_2 in the crystal growth atmosphere was controlled by a gas chromatograph "Crystal 2000M".

The crystallization rate was 2–2.5 mm/h. In the capacity of raw material we used fragments of sapphire crystals and TiO_2 powder of ≈ 10^{-3} wt. % purity. During the growth of some crystals there was used $Al_2O_3 + TiO_2$ raw material preliminarily reduced by thermal treatment in Ar + CO + H_2 atmosphere for 20 h at a temperature of 2000 K. The growth of Al_2O_3 and Al_2O_3:Ti with CTR performed using ≈ 0.1–1 wt. % of fine-dispersed graphite or Al_4C_3. CTR was realized during 5 h in Ar atmosphere (1.1–1.3·10^5 Pa) at a temperature of 2000 K.

3. Results and discussion

The present study included thermodynamic analysis and comparison of the values of the pressure of partial oxygen (P_{O_2}) in the vapor phase of Ti:sapphire under the

real conditions of the growth of crystals with the corresponding values of the region of stability for different phases in the system $TiO–TiO_2$ (Fig. 1). The changes in the thermodynamic potential ΔG^0 per O_2 mole resulting from successive oxidation

$$Ti \rightarrow TiO \rightarrow Ti_2O_3 \rightarrow Ti_3O_5 \rightarrow$$
$$\rightarrow Ti_4O_7 \rightarrow Ti_nO_{2n-1} \rightarrow TiO_2$$

were calculated using the reference data [9–11]. The pressure of molecular oxygen ($P_{O_2}^s$) in the vapor phase of Al_2O_3 in the low-pressure $CO + H_2$ atmosphere and $Ar + CO + H_2$ atmosphere with a total pressure of $1.1 \cdot 10^5$ Pa was calculated according to the procedure described in detail in [6, 12]. Under the said conditions, $P_{O_2}^s$ above Al_2O_3 melt of non-stoichiometric composition is presented by the expression:

$$P^s_{O_2} \sim (F_1 + F_2 \cdot P_{CO} + F_3 \cdot P_{H_2})^{-2/5}, \quad (3)$$

where F_1, F_2, F_3 are the functions of several parameters, including the temperature and the total pressure of the medium. For $P_{O_2}^s$ calculations we used the reference data [9, 13, 14]. If the concentration of titanium in Ti:sapphire is lower than 1 wt. %, it should be assumed that the pressure of oxygen in the vapour phase of Ti:sapphire to a sufficient accuracy coincides with the one in the vapour phase of Al_2O_3.

As seen from the results presented in Fig. 1, at the melting temperature of Al_2O_3 the region of stable existence of the phase Ti_2O_3 corresponds to the values of oxygen potential $R \cdot T \cdot \ln(P_{O_2}) < -410$ kJ/mole, i.e. the partial pressure of molecular oxygen above the system $P_{O_2} < 6 \cdot 10^{-5}$ Pa. Shown in the figure is the region of calculated values $R \cdot T \cdot \ln(P_{O_2}^s)$ limited by the real conditions of the growth of Ti:sapphire (the medium $CO + H_2$, $P_{CO} + P_{H_2} = 13$ Pa, $P_{H_2}/P_{CO} = 0.01$; the atmosphere $Ar + CO + H_2$, $P_{CO} + P_{H_2} = 400$ Pa, $P_{H_2}/P_{CO} = 1$). Under such conditions Ti_3O_5 (with the mixed charge state Ti^{3+}, Ti^{4+}) is a stable phase. The values of $P_{O_2}^s$ corresponding to the region of stable existence for the phase Ti_2O_3, can be obtained only at lower partial pressures of oxygen above Al_2O_3 melt, that is hardly realized technologically.

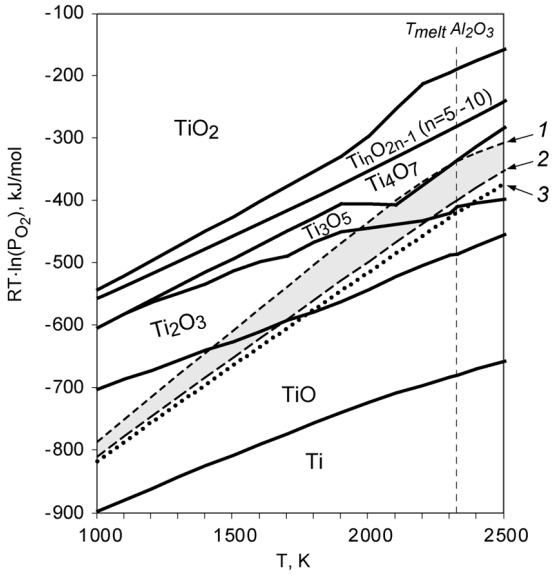

Fig. 1. Ellingham diagram for Ti–O system. Grey color denotes the region of real conditions during the growth of Ti:sapphire. *1* — $P_{CO} + P_{H_2} = 13$ Pa, $P_{H_2}/P_{CO} = 0.01$; *2* — $P_{Ar + CO + H_2} = 1.1 \cdot 10^5$ A, $P_{CO} + P_{H_2} = 400$ Pa, $P_{H_2}/P_{CO} = 1$; *3* — $P_{Ar + CO + H2} = 1.1 \cdot 10^5$ A, $P_{CO} + P_{H_2} = 1600$ Pa, $P_{H_2}/P_{CO} = 1$.

Thus, the performed estimations do not predict the possibility to provide an effective reduction of Ti^{4+} concentration during the growth of Ti:sapphire crystals. At the same time, these estimations show that at lower temperatures the region of stable existence for the phase Ti_2O_3 coincides with the region of calculated values of $R \cdot T \cdot \ln(P_{O2})$ above Ti:sapphire. In other words, it should be expected that preliminary thermal treatment of the raw material, or post-growth annealing of the crystal under the said conditions will make it possible to decrease the concentration of Ti^{4+}. To analyze the conditions of CTR it was necessary to consider possible reactions of Al_2O_3 and TiO_2 with carbon. So, we studied the thermodynamic probability of some reactions with participation of Al_2O_3, carbon and Al carbide and oxycarbides within the temperature interval from 1000 to 2000 K at different compositions of CTR medium.

In particular, there were considered the reactions leading to the formation of condensed aluminum phase (Al_{cond}) and CO, CO_2 resulting in diminution of the content of oxygen in the raw material and in violation of the stoichiometry of Al_2O_3 crystal:

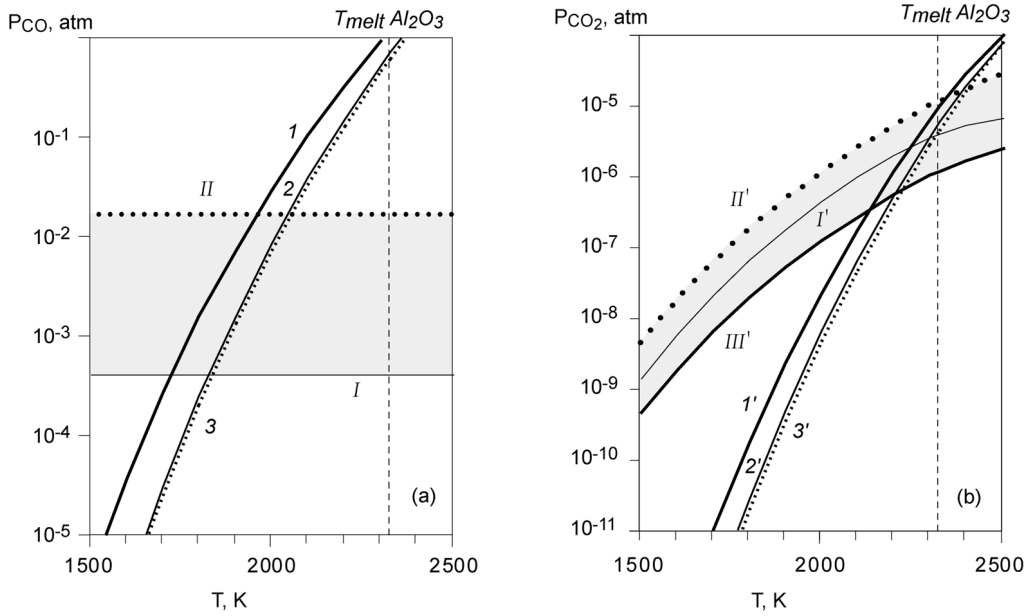

Fig. 2. Calculated temperature dependences of equilibrium pressure of gaseous products in reducing reactions with the formation of condensed Al phase: (a) *1*, *2*, *3* — P_{CO} for reactions (4, 6, 8); I, II — P_{CO} in CTR medium; (b) — *1'*, *2'*, *3'* — P_{CO_2} for reactions (5, 7, 9); *I'*, *II' III'* — calculated values of $P_{CO_2}^{s}$ above Al_2O_3 in the media $P_{CO} + P_{H_2} = 40$ Pa, $P_{H_2}/P_{CO} = 0.01$, Ar + CO + H_2, $P_{CO} + P_{H_2} = 1600$ Pa, $P_{H_2}/P_{CO} = 1$, $P_{CO} + P_{H_2} = 40$ Pa, $P_{H_2}/P_{CO} = 1$, respectively.

$$1/3Al_2O_3 + C \leftrightarrow 2/3Al_{cond.} + CO\uparrow, \quad (4)$$

$$2/3Al_2O_3 + C \leftrightarrow 4/3Al_{cond.} + CO_2\uparrow, \quad (5)$$

$$1/3Al_2O_3 + 1/3Al_4C_3 \leftrightarrow 2Al_{cond.} + CO\uparrow, \quad (6)$$

$$2/3Al_2O_3 + 1/3Al_4C_3 \leftrightarrow 8/3Al_{cond.} + CO_2\uparrow, \quad (7)$$

$$1/4Al_4O_4C + 1/4Al_4C_3 \leftrightarrow 2Al_{cond.} + CO\uparrow, \quad (8)$$

$$1/2Al_4O_4C + 1/6Al_4C_3 \leftrightarrow 8/3Al_{cond.} + CO_2\uparrow, \quad (9)$$

The ones followed by the formation of Al carbide and oxycarbides and CO, CO_2 subsequently leading to reactions (6)–(9):

$$1/3Al_2O_3 + 3/2C \leftrightarrow 1/6Al_4C_3 + CO\uparrow, \quad (10)$$

$$2/3Al_2O_3 + 2C \leftrightarrow 1/3Al_4C_3 + CO_2\uparrow, \quad (11)$$

$$1/2Al_2O_3 + 3/2C \leftrightarrow 1/2Al_2OC + CO\uparrow \quad (12)$$

$$Al_2O_3 + 2C \leftrightarrow Al_2OC + CO_2\uparrow, \quad (13)$$

$$Al_2O_3 + 3/2C \leftrightarrow 1/2Al_4O_4C + CO\uparrow, \quad (14)$$

$$Al_2O_3 + 2C \leftrightarrow Al_4O_4C + CO_2\uparrow, \quad (15)$$

$$1/4Al_4O_4C + 3/2C \leftrightarrow 1/4Al_4C_3 + CO\uparrow, \quad (16)$$

$$1/2Al_4O_4C + 2C \leftrightarrow 1/2Al_4C_3 + CO_2\uparrow, \quad (17)$$

$$Al_2OC + 3/2C \leftrightarrow 1/2Al_4C_3 + CO\uparrow, \quad (18)$$

$$2Al_2OC + 2C \leftrightarrow Al_4C_3 + CO_2\uparrow. \quad (19)$$

The reactions resulting in the formation of Al_{cond} with subsequent violation of Al_2O_3 stoichiometry (4)–(9) and then leading to $Ti^{4+} \rightarrow Ti^{3+}$ reduction according to the scheme:

$$(V_O^{++} + 2e) + Ti^{4+} \leftrightarrow (V_O^{++} + e) + Ti^{3+}, \quad (20)$$

where $(V_O^{++}) + 2e$ is a neutral *F*-center; $(V_O^{++}) + e$, F^+-center.

The reactions resulting in the formation of gaseous products of Al_2O_3 dissociation:

$$Al_2O_3 + C \leftrightarrow (Al_g, AlO, Al_2O)\uparrow + (CO, CO_2)\uparrow \quad (21)$$

do not increase the degree of Al_2O_3 non-stoichiometry, they only raise the evapora-

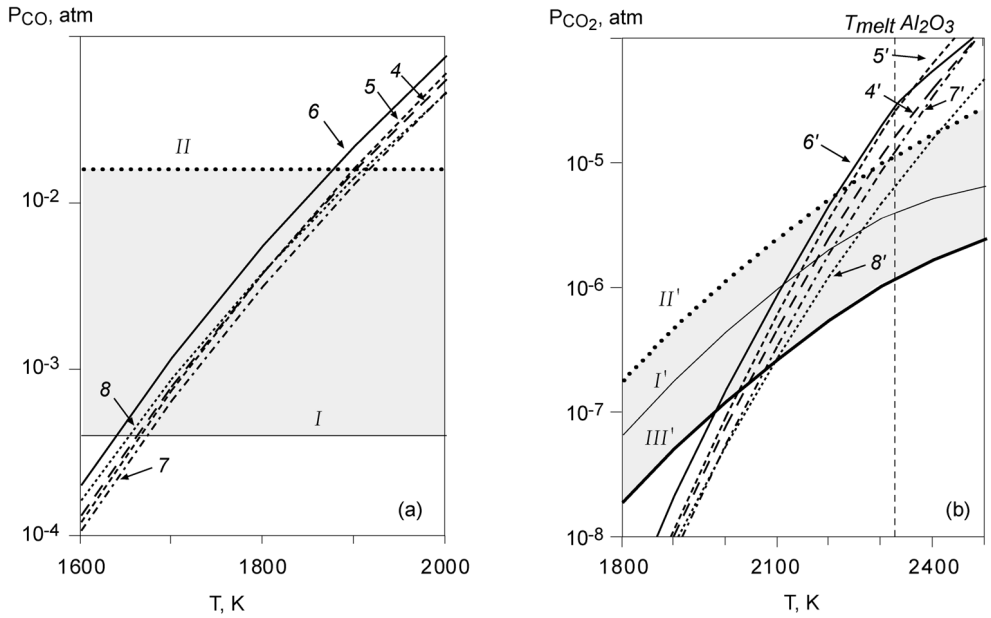

Fig. 3. Temperature dependences of equilibrium pressure of gaseous products in reducing reactions with the formation of Al carbide and oxycarbides. (a) (6) — (10) — P_{CO} for reactions (10), (12), (14), (16), (18); I, II — P_{CO} CTR medium; (b) (4') — (8') — P_{CO_2} for reactions (11), (13), (15), (17), (19); I', II' III' — calculated $P_{CO_2}{}^s$ values in the media $P_{CO} + P_{H_2} = 40$ Pa, $P_{H_2}/P_{CO} = 0.01$, Ar + CO +H_2, $P_{CO} + P_{H_2} = 1600$ Pa, $P_{H_2}/P_{CO} = 1$, $P_{CO} + P_{H_2} = 40$ Pa, $P_{H_2}/P_{CO} = 1$, respectively.

tion rate. Therefore, these reactions are excluded from further analysis.

The temperature dependences of equilibrium pressure for the gaseous products (CO, CO_2) of the reducing reactions leading to the formation of Al_{cond} are presented in Fig. 2. Shown in Fig. 3 are the temperature dependences of the reactions resulting in the formation of Al carbide and oxycarbides. The values of equilibrium CO and CO_2 pressure are determined from the known expressions for equilibrium constants of the reactions:

$$\Delta G^0 = RT\ln K, \qquad (22)$$

where ΔG^0 is the change of the thermodynamic potential in the reaction realized under standard conditions; R, the gas constant; K, the equilibrium constant of the reaction defined by the ratio of the partial pressures of the reaction products and the reagents; for reactions (2)–(17) it corresponds to P_{CO} or P_{CO_2}. The changes in the thermodynamic potential ΔG^0 per 1 mole of CO, CO_2 were calculated using the reference data [13, 14] and the data from [15] for aluminium carbide and oxycarbides.

Shown in Fig. 2a and 3a are the regions of P_{CO} values in the CTR medium $CO + H_2$, $P_{CO} + P_{H_2} = 40$ Pa (curve I) and in the atmosphere $Ar + CO + H_2 = 1600$ Pa (curve II). Fig. 2b and 3b present the calculated $P_{CO2}{}^s$ values in the gas phase above Al_2O_3 melt, in the CTR medium $CO + H_2$, $P_{CO} + P_{H2} = 40$ Pa, $P_{H2}/P_{CO} = 1$ (curve III') and in the atmosphere $Ar + CO + H_2$, $P_{CO} + P_{H2} = 1600$ Pa, $P_{H2} + P_{CO} = 1$ (curve II'). Under such conditions $P_{CO2}{}^s$ value essentially differs from the equilibrium value above graphite and is defined by the equilibrium condition of the reaction

$$CO + 1/2O_2 \leftrightarrow CO_2 \qquad (23)$$

above corundum obtained from the expression:

$$P_{CO_2}{}^s = \left(P_{CO_2}{}^s\right) \cdot P_{CO} \cdot K_{CO_2}, \qquad (24)$$

where P_{CO_2} *is defined by dependence (3),* K_{CO_2} is the constant of reaction (23). The value of $P_{CO_2^s}$ was calculated using the reference data [14, 18, 19].

As seen while comparing the regions of real composition of the CTR medium with the values of equilibrium pressure P_{CO} and P_{CO_2} for reactions (4)–(19), the considered

Table 1. Calculated values of onset temperature for reactions (2)–(17) at different composition of the medium in crystallization chamber

Number of reaction (denotation of curve in Fig. 2,3)	Composition of medium		Number of reaction (denotation of curve in Fig. 2, 3)	Composition of medium		
	P_{CO} = 40 Pa	P_{CO} = 1600 Pa		$P_{CO} + P_{H2}$ = 40 Pa P_{H2}/P_{CO} = 1	$P_{CO} + P_{H2}$ = 40 Pa P_{H2}/P_{CO} =0.01	$P_{CO} + P_{H2}$ = 1600 Pa P_{H2}/P_{CO} = 1
2(1)	1723	1956	3(1')	2135	2250	2342
4(2)	1826	2043	5(2')	2202	2300	2390
6(3)	1837	2054	7(3')	2225	2320	2405
8(4)	1662	1902	9(4')	2043	2175	2282
10(5)	1665	1898	11(5')	2023	2145	2236
12(6)	1638	1876	13(6')	1980	2115	2212
14(7)	1673	1915	15(7')	2074	2207	2313
16(8)	1654	1910	17(8')	2095	2264	2408

reactions are thermodynamically probable starting from temperatures lower than the melting point. The onset temperatures for the reactions leading to the formation of CO are lower than those for the reactions resulting in the formation of CO_2. With the increase of P_{CO} in the crystal growth medium the reaction onset temperature rises, too. At the same time, the onset temperature for the reactions with CO_2 formation also depends on the value of P_{H_2}/P_{CO} ratio in the medium, that is bound up with dependences (3) and (24). The calculations of the reaction onset temperatures at different compositions of the medium in the crystallization chamber are presented in Table 1. As follows from the results shown in Fig. 2, 3 and Table 1, in the presence of carbon and Al_4C_3 in the raw material the reduction efficiency rises as P_{CO} value in the crystallization chamber decreases. This can be successfully achieved at lower pressures of the medium. However, in this case it is necessary to take into account an essential increase of evaporation rate for the raw material and the melt according to reactions (21). Moreover, the calculations show that in the presence of carbon in the raw material, the reduction processes leading to the formation of condensed Al phase which give rise to violation of stoichiometry in Al_2O_3, start at temperatures higher than those for the reactions with the formation of Al carbide and oxycarbides. Therefore, one may expect that the presence of carbon and Al_4C_3 will exert equivalent action on the reduction process. Further it will be shown that, according to experimental studies, the intensities of the absorption bands bound up with the presence of F- and Ti^{4+}-centers in the optical spectra of Al_2O_3:Ti crystals grown with CTR do not acquire noticeable changes at introduction of graphite or Al_4C_3 in the raw material. The presence of carbon in the raw material also facilitates the reduction of titanium oxides with subsequent formation of lower oxide and gaseous products of CO, CO_2 according to the reactions:

$$4TiO_2 + C = Ti_4O_7 + [CO]\uparrow, \quad (25)$$

$$8TiO_2 + C = 2Ti_4O_7 + [CO_2]\uparrow, \quad (26)$$

$$3Ti_4O_7 + C = 4Ti_3O_5 + [CO]\uparrow, \quad (27)$$

$$6Ti_4O_7 + C = 8Ti_3O_5 + [CO_2]\uparrow, \quad (28)$$

$$2Ti_3O_5 + C = 3Ti_2O_3 + [CO]\uparrow, \quad (29)$$

$$4Ti_3O_5 + C = 6Ti_2O_3 + [CO_2]\uparrow, \quad (30)$$

$$Ti_2O_3 + C = 2TiO + [CO]\uparrow, \quad (31)$$

$$2Ti_2O_3 + C = 4TiO + [CO]\uparrow. \quad (32)$$

The temperature dependences of the equilibrium pressure of CO, CO_2 in these reactions are presented in Fig. 4. The calculations of the changes in the thermodynamic potential ΔG^O per 1 mole of CO, CO_2 due to the reaction of successive reduction $TiO_2 \rightarrow Ti_nO_{2n-1} \rightarrow Ti_4O_7 \rightarrow Ti_3O_5 \rightarrow Ti_2O_3 \rightarrow TiO$ were made using the reference data [10, 11, 13]. As well as in the case of reactions (4)–(19), the equilibrium pressure of

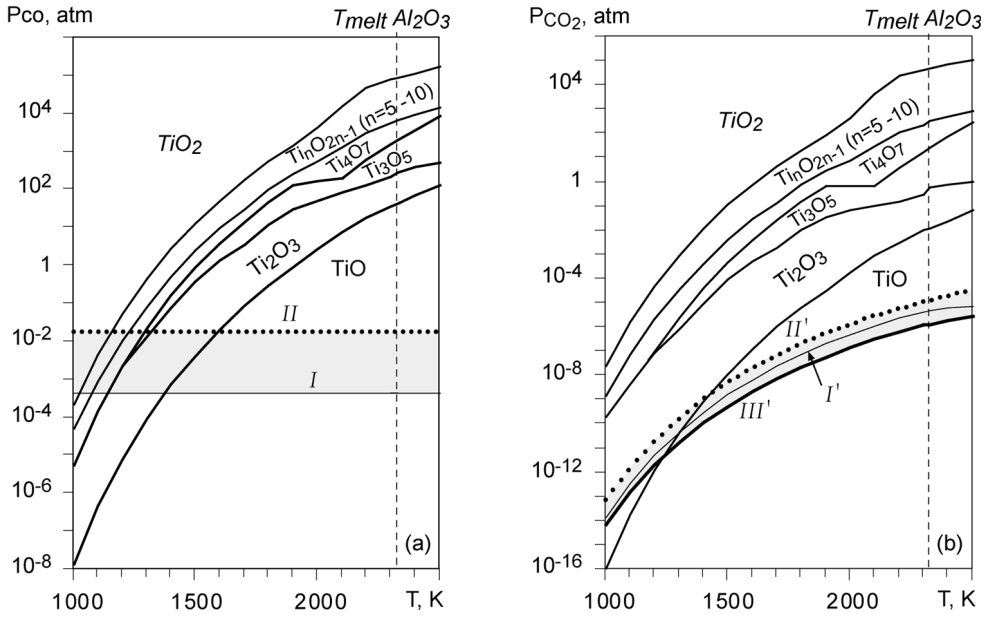

Fig. 4. Temperature dependences of equilibrium pressure of CO (a) and CO_2 (b) at reduction of titanium oxides with/by carbon. I, II — P_{CO} in the growth medium; I', II' III' — calculated P_{CO2}^{s} qvalues in the medium $P_{CO} + P_{H2} = 40$ Pa, $P_{H2}/P_{CO} = 0.01$, Ar + CO+H_2, $P_{CO} + P_{H2} = 1600$ Pa, $P_{H2}/P_{CO} = 1$, $P_{CO} + P_{H2} = 40$ Pa, $P_{H2}/P_{CO} = 1$, respectively.

CO and CO_2 was determined from the expressions for the equilibrium constants of the reactions using relation (22). By analogy with Fig. 2, 3, shown in Fig. 4 are the regions of the real P_{CO} values and the calculated $P_{CO_2^s}$ values in the gas phase above Al_2O_3 limited by the values characteristic of the process of Ti:sapphire growth in the low-pressure medium ($P_{CO} + P_{H_2}$) = 40 Pa, $P_{H_2}/P_{CO} = 1$ — curve III') and in the atmosphere Ar + CO + H_2, $P_{CO} + P_{H2} = 1600$ Pa, $P_{H2}/P_{CO} = 1$ — curve II'). Likewise Fig. 1, the diagram presented in Fig. 4 characterizes the regions of stability for different phases in the system TiO–TiO_2, but in the presence of carbon and the gas phase CO or CO_2.

Let us compare the real composition of the growth medium with the values of P_{CO} and P_{CO2} equilibrium pressures for reactions (25)–(32). One can see that within the whole considered interval of the reducing medium composition these reactions, as well as reactions (4)–(9), favour intense $Ti^{4+} \rightarrow Ti^{3+}$ reduction and diminution of the relative Ti^{4+} concentration.

The obtained thermodynamic estimations, in particular, the reaction onset temperature, as well as the experimental data for the growth of Al_2O_3:C crystals were used for the growth of Al_2O_3:Ti with CTR.

Fig. 5 presents the optical absorption spectra of the standard (nominally pure) crystals of sapphire containing $\approx 7 \cdot 10^{-4}$ wt % of residual titanium additive and of Ti:sapphire with ≈0.06 wt % titanium content grown in Ar + CO + H_2 atmosphere, $P_{CO} + P_{H2}$ ~ 400 Pa, $P_{H2}/P_{CO} = \approx 0.1$, in $P_{CO} + P_{H2} \approx 7$ Pa atmosphere, as well as the spectra of Al_2O_3 and Al_2O_3:Ti crystals with CTR.

As shown by investigations, the optical characteristics of such crystals essentially depend on the partial pressure of the reducing components (P_{CO}, P_{H2}) at all the stages of the crystallization process, as well as on the concentration of polyvalent titanium additive in the raw material. If the crystal growth conditions provide the transition of a considerable portion of titanium into the charge state Ti^{3+}, then the absorption band of neutral *F*-centers (~ 205 nm) is dominating in the UV-region. If the growth conditions do not provide such a transition, then the said spectral region contains the dominating broad non-elementary band at 200–250 nm bound up with the presence of titanium in the charge state Ti^{4+}. As seen from Fig. 5, such a spectrum is characteristic of sapphire grown in a low-pressure medium (curve *2*). At the same time, the absorption band of neutral *F*-centers prevails in the spectra of the nominally pure crystals grown in the atmosphere Ar + CO + H_2

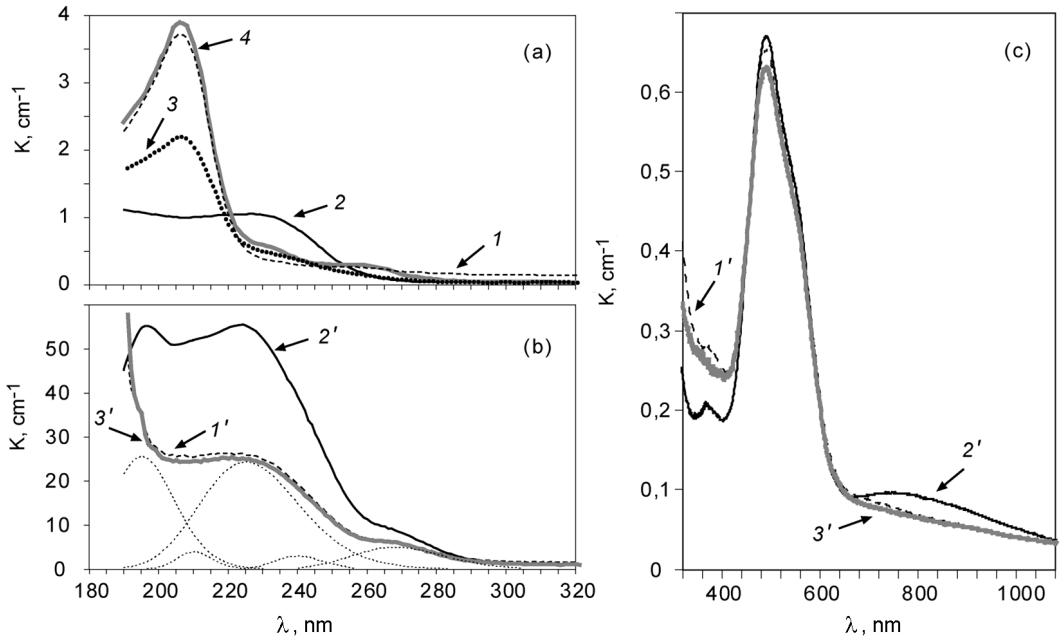

Fig. 5. Optical absorption spectra for sapphire with ≈$7\cdot10^{-4}$ wt% residual titanium content (a) and Ti:sapphire containing ≈0.06 wt% of titanium (b) grown in the media ≈0.1 (1), (1') and $P_{CO} + P_{H2} \approx 7$ Pa, (2), (2'), and the spectra for the crystals grown in the medium $P_{CO} + P_{H2} \approx 7$ Pa from the raw material containing ≈0.3 wt% of C (3), ≈1 wt% of C (3') and ≈1 wt% of Al_4C_3 (4). In Fig.5(b) dotted lines show decomposition of the spectrum (3') into Gaussian components.

(curve *1*), as well as in the ones of Al_2O_3:C crystals grown in a low-pressure medium (curve *3, 4*). In other words, the presence of additional inner source of reduction exerts the same influence on the process of titanium reduction as a considerable increase of the reduction potential of the crystal growth medium. It should be also noted that, in comparison with the nominally pure crystals, Al_2O_3:C crystals contain a considerably higher concentration of F^+-centers (the bands at ~ 230 and ~ 260 nm). It has been assumed that the formation of elevated concentration of F^+-centers in such crystals is caused by substitution of trivalent Al cation by bivalent carbon ion, and by the formation of F^+-center as a compensator of C^{2+} charge [16, 17]. Along with the above-said widespread viewpoint, there exists an alternative assumption to the effect that carbon in Al_2O_3:C crystal is an anionic additive, and F^+-centers function as C^{4-} charge compensators in the O^{2-} position in Al_2O_3 lattice [18]. Irrespective of the mechanism of F^+-center formation, the character of the spectra of Al_2O_3:C crystals (curves *3, 4* in Fig. 5) testifies that during the growth of these crystals C and Al_4C_3 are not consumed completely as a result of reactions (4)–(9) and (25)–(32): they are partially dissolved in the crystal and influence its optical characteristics.

In the UV-region the optical absorption spectrum of Al_2O_3:Ti crystal grown in the low-pressure medium (curve *2'*) contain the characteristic absorption band at 200–250 nm bound up with Ti^{4+}. Its intensity is observed to essentially diminish with the rise of the reduction potential of the growth medium (curve *1'*), as well as for Al_2O_3:Ti crystals with CTR (curve *3'*). The absorption in the band at ~ 800 nm related to the presence of Ti^{3+}–Ti^{4+} centers in the crystal also decreases (Fig. 5c).

Preliminary studies show that the same effect is also observed at introduction of Al_4C_3 into the raw material. The optical absorption spectra allowed to estimate the values of $[Ti^{4+}]/\{Ti^{3+}]$ in Al_2O_3:Ti crystals and in the ones with CTR (Table 2).

The concentration of Ti^{4+} was estimated from the intensity of the absorption band with a maximum at 225 nm bound up with the presence of Ti^{4+} according to the Smakula's formula:

$$[Ti^{4+}] \cdot f = 0.87 \cdot 10^{17} \cdot n \cdot (2 + n^2)^{-2} \cdot K_{max} \cdot \Delta, \text{cm}^{-3}, \quad (33)$$

where K_{max} is the absorption coefficient; Δ, the peak width at the half-intensity; n, the refractive index at the wavelength corre-

Table 2. Growth conditions for Al_2O_3:Ti and Al_2O_3:Ti crystals with CTR and $[Ti^{4+}]/[Ti^{3+}]$ ratio in these crystals

Number of crystal	Crystal	Composition and conditions for raw material preparation	Composition of crystal growth medium	Values of $R{\cdot}T{\cdot}\ln(P_{O2}{}^{s}$ (calculation of $P_{O2}{}^{s}$ from (1) at T = 2327 K) values	$[Ti^{4+}]/[Ti^{3+}]$ values
1	Al_2O_3:Ti	$Al_2O_3 + TiO_2$	$P_{CO} + P_{H2} \approx 7$ Pa $P_{H2}/P_{CO} \approx 0.01$	−337	0.029
2	Al_2O_3:Ti	$Al_2O_3 + TiO_2$, Thermal treatment in Ar + CO + H_2, $P = 1.3{\cdot}10^5$ Pa, $P_{CO} + P_{H2}$ ~ 400 P, $P_{H2}/P_{CO} \approx 0.01$	$P_{CO} + P_{H2} \approx 7$ Pa $P_{H2}/P_{CO} \approx 0.01$	−337	0.02
3	Al_2O_3:Ti	Al_2O_3:TiO_2	Ar + CO + H_2, P = 1.3 Pa, $P_{CO} + P_{H2}$ ~ 400 Pa, $P_{H2}/P_{CO} \approx 0.01$	−399	0.009
4	Al_2O_3:Ti:C	$Al_2O_3 + TiO_2$ + C (1 wt%)	$P_{CO} + P_{H2}$ ~ 7 Pa $P_{H2}/P_{CO} \approx 0.01$	−337	0.001

sponding to K_{max}; f, the oscillator strength (equal to =0.5 as in [19]). The spectral band of Ti^{4+} ions in the region of 190–310 nm containing overlapping bands of different defects such as F^+-centers (the bands with maxima at 230 and 260 nm), was singled out by the Alentsev-Fock method with subsequent resolution into elementary Gaussian components (for details see [20]). The criterion of resolution accuracy was the relation [21]

$$\gamma = \frac{\sum_{i=0}^{m}\left(K_i^{\exp} - K_i^{calc}\right)^2}{\sum_{i=0}^{m}(K_i^{\exp})^2} \le 0.05, \qquad (34)$$

where m — are the points of the curve $K(\lambda)$, $K_i^{\exp}$, the experimental values; K_i^{calc}, the values calculated from the sum of $K(\lambda)$ components at the corresponding wavelength. The calculation was made for 190–310 nm range, m = 120. For the spectra presented in Fig. 4, γ amounts to $2–4{\cdot}10^{-3}$.

The concentration of Ti^{3+} was estimated using the empiric relation [22]:

$$[Ti^{3+}] = \frac{K_{514}}{18.55\text{cm}^{-1}}, \text{ wt\%}, \qquad (35)$$

where K_{514} is the coefficient of optical absorption at 514 nm wavelength.

Table 2 contains the data for the crystals which optical absorption spectra are presented in Fig. 5(b,c), as well as the data obtained for Al_2O_3:Ti crystal grown from the raw material preliminarily reduced by thermal treatment in Ar + CO + H_2 atmosphere during 20 hours at 2000 K.

As seen while analyzing these data, the said preliminary thermal treatment of the raw material makes it possible to decrease the relative content of Ti^{4+} approximately by 1.5 times, that qualitatively coincides with the estimation which follows from Fig. 1. Diminution of the oxygen potential at the growth of the crystal in Ar + CO + H_2 atmosphere and introduction of carbon into the raw material lead to practically equivalent result and allow to diminish the value of $[Ti^{4+}]/[Ti^{3+}]$ more than by 2–3 times. As seen from the optical absorption spectra (Fig. 5), such a decrease of the content of Ti^{4+} ions leads to the corresponding diminution of the absorption (by 2–3 times) in the region of 800 nm that is bound up with the activator complexes Ti^{3+}–Ti^{4+} .

4. Conclussions

Thus, the presence of the additional inner reduction source (the introduction of C or Al_4C_3) during carbothermal treatment of the raw material makes it possible to effectively diminish the value of oxygen potential which defines the relative content of the activator in the charge state Ti^{4+} and Ti^{3+}–Ti^{4+}.

References

1. P.F.Moulton, *J. Opt. Soc. Am. B.*, **3**, 125 (1986).
2. A.J.Strauss, R.E.Fahey, A.Sanchez, R.L.Aggarwal, *SPIE Laser Nonlin. Opt. Mater.*, **681**, 62 (1986).
3. A.Sanchez, A.J.Strauss, R.L.Aggarwal, R.E.Fahey, *IEEE J. Quant. Electron.*, **24**, 995 (1988).
4. R.L.Aggarval, A.Sanchez et al., *IEEE J. Quant. Electron.*, **24**, 1003 (1988).
5. N.S.Sidelnikova, S.V.Nizhankovskyi, V.V.Baranov, *Functional Materials*, **22**, 461 (2015).
6. A.Ya.Danko, V.M.Puzikov, V.P.Seminozhenko, N.S.Sidelnikova, Technological Bases of Growth of Leucosapphire in Reducing Conditions. ISMA, Kharkov (2009) [in Russian].
7. Hu Ke-Yan, Xu Jun, Wang Chuan-Yong et al., *J. Inorg. Mater.*, **27**, 1321 (2012).
8. S.V.Nizhankovskiy, A.Ya Dan'Ko, E.V. Krivonosov, V.M.Puzikov, *J. Inorg. Mater.*, **46**, 41 (2010).
9. L.V.Gurvich, I.V.Weitz, V.A.Medvedev et al., Thermodynamic Properties of Individual Substances. Reference Edition in 4 Volumes., V1, B2. Science, Moscow (1978) [in Russian].
10. L.V.Gurvich, I.V.Weitz, V.A.Medvedev et al., Thermodynamic Properties of Individual Substances. Reference Edition in 4 Volumes., V4, B2, Science, Moscow (1978) [in Russian].
11. M.Cancarevic, M.Zinkevich, F.Aldinger, *Computer Coupling of Phase Diagrams and Thermochemistry*, **31**, 330 (2007).
12. A.Ya.Danko, N.S.Sidelnikova, *Functional Materials*, **8**, 271 (2001).
13. L.V.Gurvich, I.V.Weitz, V.A.Medvedev et al., Thermodynamic Properties of Individual Substances. Reference Edition in 4 Volumes, V2, B2, Science, Moscow (1978) [in Russian].
14. L.V.Gurvich, I.V.Weitz, V.A.Medvedev et al., Thermodynamic Properties of Individual Substances. Reference Edition in 4 Vol., V3, B2, Science, Moscow (1981) [in Russian].
15. J.-M.Lihrmann, J.Tirlocq, P.Descamps, F.Cambier, *J. Eur. Ceramic Soc.*, **19**, 2781 (1999).
16. M.S.Akselrod, V.S.Kortov, D.J.Kravetsky, V.I.Gotlib, *Radiat. Prot. Dosim.*, **32**, 15 (1990).
17. X.Yang, H.Li, Y.Cheng et al., *J. Cryst. Growth*, **310**, 3800 (2008).
18. X.Yang, J.Li, Q.Y.Bi et al., *J. Appl. Phys.*, **104**, 1 (2008).
19. N.A.Moskvin, V.A.Sandulenko, E.A.Sidorova, *J. Appli. Spectrosc.*, **32**, 1017 (1980).
20. S.V.Nizhankovskii, N.S.Sidel'nikova, V.V.Baranov, *Phys. Solid State*. **57**, 763 (2015).
21. V.G.Tyazhelova, *J. Appl. Spectr.*, **10**, 22 (1969).
22. J.Stone-Sundberg, M.Kokta, A.Silberstein et al., Workshop: Technological Bottlenecks in CHISP Lasers, Paris, April 1-4, (2003).